

Estimation of Velocity of the Polar Record Glacier, Antarctica Using Synthetic Aperture Radar (SAR) [†]

Prashant H. Pandit ^{1,*}, Shridhar D. Jawak ² and Alvarinho J. Luis ²

¹ Department of Natural Resources, TERI University, New Delhi 110 070, India

² Polar Remote Sensing Section, Polar Sciences Group, Earth System Science Organization (ESSO), National Centre for Antarctic and Ocean Research (NCAOR), Ministry of Earth Sciences (MoES), Government of India, Headland Sada, Vasco-da-Gama, Goa 403804, India; shridhar.jawak@gmail.com (S.D.J.); alvluis1@gmail (A.J.L.)

* Correspondence: prashant.pandit@outlook.com; Tel.: +91-886-078-7847

[†] Presented at the 2nd International Electronic Conference on Remote Sensing, 22 March–5 April 2018; Available online: <https://sciforum.net/conference/ecrs-2>.

Published: 22 March 2018

Abstract: The ice flow velocity is a critical variable in understanding the glacier dynamics. The Synthetic Aperture Radar Interferometry (InSAR) is a robust technique to monitor Earth's surface mainly to measure its topography and deformation. The phase information from two or more interferogram further helps to extract information about the height and displacement of the surface. We used this technique to derive glacier velocity for Polar Record Glacier (PRG), East Antarctica, using Sentinel-1 Single Look Complex images that were captured in Interferometric Wide mode. For velocity estimation, Persistent Scatterer interferometry (PS-InSAR) method was applied, which uses the time coherent of permanent pixel of master images and correlates to the same pixel of the slave image to get displacement by tracking the intensity of those pixels. C-band sensor of European Space Agency, Sentinel-1A, and 1B data were used in this study. Estimated average velocity of the PRG is found to be approximately $\approx 400 \text{ m a}^{-1}$, which varied from ≈ 100 to $\approx 700 \text{ m a}^{-1}$. We also found that PRG moves at ≈ 700 and 200 m a^{-1} in the lower part and the upper inland area, respectively.

Keywords: PS-Interferometry; velocity; Sentinel-1; Polar Record glacier; microwave remote sensing

1. Introduction

Synthetic Aperture Radar interferometry (InSAR) is the common practice for the measurement of topography and deformation of the earth surface. It is an active microwave radar imaging system that is based on the Doppler motion principle, wherein two Synthetic Aperture Radar (SAR) images are used to generate an interferogram. It uses InSAR acquiring great capabilities to measure and to detect ground surface deformation up to sub-centimeter level on a wide scale. Several studies that were based on InSAR have quantified earth surface deformation caused by processes, like ice motion, subsidence phenomena, earthquake, volcanism, etc. While Radio Detection and Ranging (RADAR) is one of the primary tools that measures distance of object, SAR records phase, and amplitude information; the phase of the radar represents the number of cycles of oscillation of waves between radar and the object's surface. If phase is not provided, it is singular image, for which more than one image is required for processing, however, by the convention, the amplitude or intensity of images are usually delivered to the end user.

The application of the SAR techniques for cryosphere is increasingly day by day for different purposes, such as measurement of the flow of glacier and ice sheet, generation of high resolution topographic maps, and the calculation of surface displacement that is associated with crustal deformation [1]. Rapid movement of the flowing ice creates spectacular fringes pattern in interferogram,

which increases with the increase in the surface velocity that sometimes exceeds more than 1 m/day. Monitoring such high motion by satellite radar interferometry needs small orbital and temporal separation between consecutive passes [2]. Sequence of differential interferogram such as Differential SAR interferometry (DInSAR or DiffSAR), is an effective technique to explore the properties of InSAR for monitoring the temporal behavior for the change detection, which leads to the generation of the time series for monitoring deformation [3]. The temporal gap of repeat-pass interferometry with marginal repetition of days, months, or even years can be used to monitor long-term geodynamic phenomenon. DInSAR measures the displacements with centimeter accuracy that provided higher coherence is available. Persistent or Permanent Scatterer Interferometry (PS Interferometry) allows for monitoring the subsidence effect with millimeter accuracy. The processing system of PSI was developed to cope with a single dominant point scattered within a resolution cell; when the number of interferogram increases the density of permanent scattering also improves.

The recognition and quantification of the glacier surface deformation using the SAR interferometry technique have great impact on the accuracy of results. Phase difference between two SAR images that were taken with some temporal gap with a different view angle has been used to measure the velocity of the ice sheets and the movement of glaciers in the polar region, as well as the Himalayan cryosphere. InSAR phase is sensitive to both coherent displacement and surface topography along the SAR look vector that was derived from the acquisitions of the InSAR image pair [4]. Coherence tracking and intensity tracking are two cross-correlation techniques that were applied to SAR data to produce two-dimensional (2D) vector field datasets with InSAR. If two or more radar images with good correlation and orbital, topographic, and tropospheric contributions are modelled, the precision of InSAR of the order of millimeter can be achieved; however, other errors may arise, while resolving the phase ambiguity through the unwrapping process [5]. The coherence over the glacier surface is affected by flow condition and meteorological forcing, which diminishes with increasing the time interval between the SAR images that were used to generate interferogram. Meteorological parameters, which create decorrelation, include the surface melt of snow and ice due to rise in surface temperature, precipitation in the form of snowfall, and sometimes winds redistribute snow and ice. Decorrelations that are caused by the glacier motion are incoherent displacements of adjacent scatterers and rapid flow if local deviations from the overall images registration function are not considered [6].

2. Experiments

2.1. Study Area and Data Used

The Polar Record Glacier (PRG) (as shown in Figure 1) is located 69.5° S, 75.4° E (Figure 2) on Princess Elizabeth land. It is one of the largest outlet glacier flow that is situated near Larsemann Hills in East Antarctica. It is one of the outlet glaciers besides the Ingrid Christensen coast that is bounded by Dodd Island and Meknattane Nuntaks [7]. The Indian Antarctic Research station Bharati is located to the northeast, about 50 km from this glacier. Using satellite data from 1937 to 1947, Roscoe, a geographer in the United States (US), detected an ice tongue extending ~ 70 km into the open sea and he predicted that the tongue would calve when it encounters Amery Ice Shelf (AIS) which was confirmed that a large ice piece broke away into the sea between 1980–1990. Further monitoring has revealed that the total area is decreasing every year: from 450 km² it decreased to 300 km² after several calving events. Ref. [8] claimed that the surface velocity of the tongue enhanced by 19% from 140 to 580 m a⁻¹ in winter to 720 m a⁻¹ in the summer.

In this study, we used Sentinel-1 SAR interferometric single look complex data (SLC) level-1 product. More specification of the data set that was used in this study is mentioned in Tables 1 and 2.

Table 1. Specification of Sentinel-1 product used in this study.

Parameters Specification	Parameters Specification
Polarization	HH
Incidence angle	31°–46°
Azimuth Resolution	20 m
Ground range resolution	5 m
Azimuth and Rang look	Single
Swath	250 km
Phase Error	5°

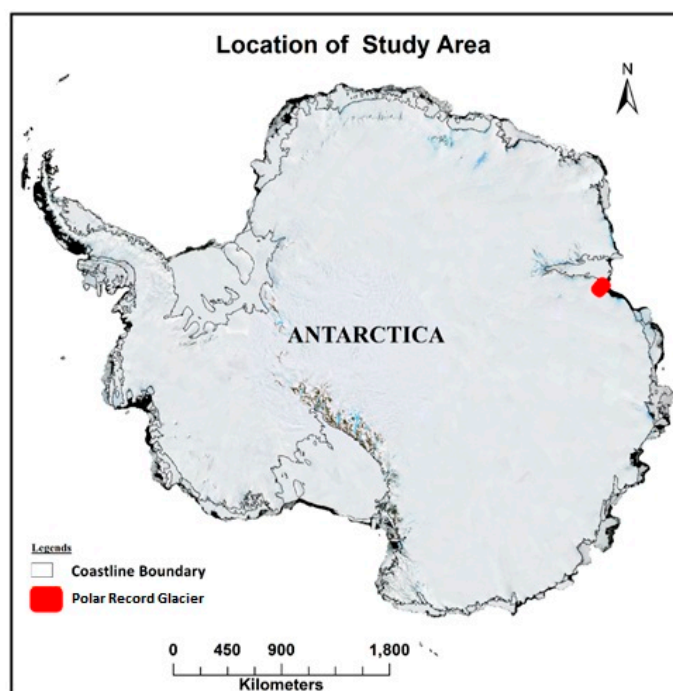


Figure 1. Location of Polar Record Glacier (PRG) East Antarctica.

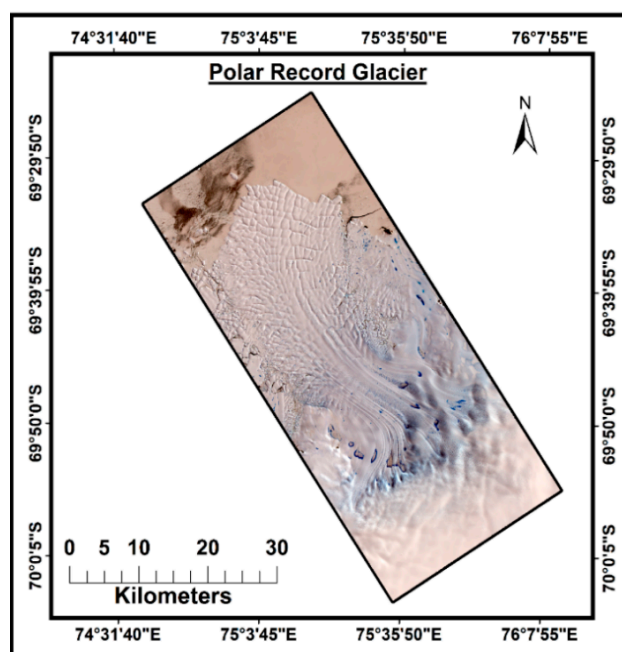


Figure 2. False Color Composition Map for PRG.

Table 2. Data used in study of PRG glacier.

Mission	Acquisition Date	Orbit Number	Id	Unique Identifier	Flight Direction
S1A	07-08-2016	012500	0138DA	DA1D	Descending
S1A	19-08-2016	012675	013E9C	7FB2	Descending
S1A	31-08-2016	012850	01448E	27DE	Descending
S1A	12-09-2016	013025	014A22	2258	Descending
S1A	18-10-2016	013550	015B08	93BF	Descending
S1A	11-11-2016	013900	0165F4	9EDC	Descending
S1A	05-12-2016	014250	0170BC	4526	Descending
S1A	29-12-2016	14600	017BB9	C3E0	Descending
S1A	22-01-2017	014950	018671	6B79	Descending
S1B	30-09-2016	002304	003E57	540C	Descending
S1B	24-10-2016	002654	0047CC	A1F8	Descending
S1B	05-11-2016	002829	004CA8	F585	Descending
S1B	17-11-2016	003004	0051B4	7BAB	Descending
S1B	11-12-2016	003354	005BA9	C91B	Descending
S1B	04-01-2017	003704	0065D5	6C7B	Descending
S1B	21-02-2016	004404	007A9F	C99D	Descending

2.2. Methodology

Interferometric processing of SAR data for Digital Elevation Model (DEM) generation, as well as velocity calculation, involves common steps: Image Co-registration, Interferogram Generation, Interferogram flattening and topographical phase removal, Phase Unwrapping, velocity conversion, and Geocoding [9–13].

Processing Steps for Velocity Calculation

For the velocity calculation of study area, we used the PSInSAR method where all of the SAR single look complex (SLC) images were involved for co-registration. As mentioned earlier, in the PSI method the number of images affects the accuracy of the results because the co-registration depends upon the amplitude of the signal [14]. The SARPROZ software that was used to generate the velocity map from the SAR data, has its own inbuilt module to handle every step of the functions, and the function is further parted in sub-function, as shown in Figure 3.

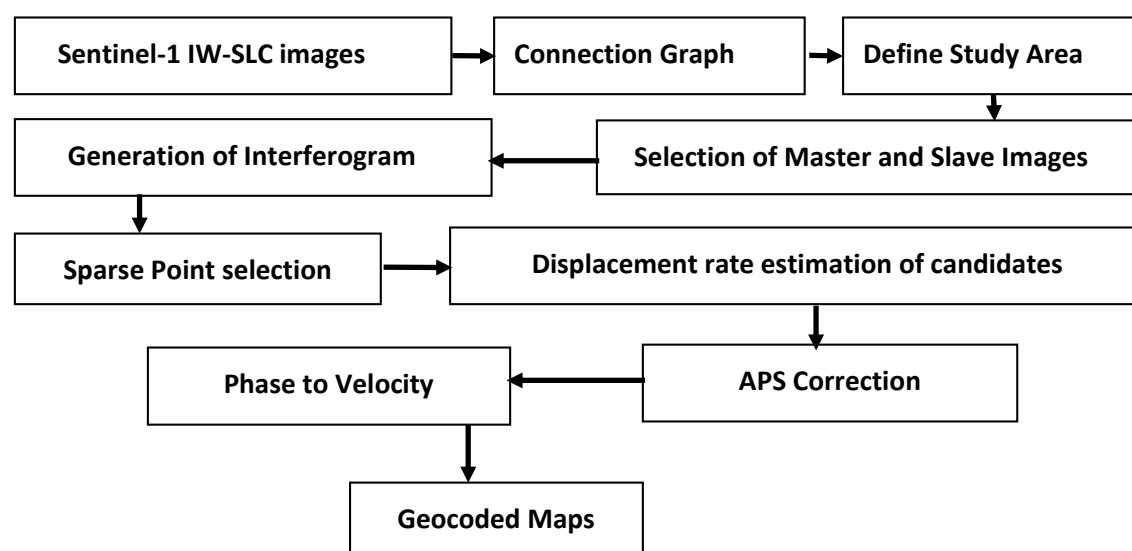


Figure 3. General steps for Persistent Scatterer Interferometric process.

First, SLC images were co-registered for Terrain Observation by Progressive Scans (TOPS), which is a Sentinel-1 image capturing mode (for sentinel-1 TOPS Co-registration). At the time of registration of images, we also used DEM (for terrain correction) and Precise orbit information. In second step, the selection of Master and Slave images was incorporated depending on the need and

availability. Before performing the third step, sparse point selection based on amplitude stability and reflective maps was carried. These sub-processes, along with synthetic GCP generation, were performed using RAMP DEM, which were uploaded with the software. In final step of data processing, geocoding process was processed.

3. Results and Discussion

The velocity of the Polar Record glacier is calculated with the help of sixteen SAR images using the PSInSAR process. All of the 16 images are alternatively used as master and slave, if one image is master rest of other images behave as slave. In this study, we found similar behavior from image, if the coherence of master and slave is higher, and then accuracy was higher. We also found that PRG is one of the very fast-moving glacier in eastern part of Antarctic with annual velocity of ≈ 700 m for lower part and ≈ 200 m for the upper inland area. The western part of the glacier is moving faster in comparison with the eastern part. The rate of glacier movement in summer was found to be more than 4 mday^{-1} , whereas some inland region exhibited 2 mday^{-1} .

4. Conclusions

It is possible to find the velocity of the glacier using C-band sensor satellite with an accurate result. Polar Record glacier is very fast flowing glacier. The velocity of PRG was estimated to be around 2 mday^{-1} for the tongue portion and nearly 1 mday^{-1} at upper inland area. The results showed that at lower altitude the velocity was $700\text{--}750 \text{ ma}^{-1}$, whereas at higher altitude toward eastern side of the glacier flow, it was $300\text{--}400 \text{ ma}^{-1}$. In the PSInSAR method on Interferometric SAR data for estimating glacier velocity, the accuracy of the results varied according to the coherence level of the SAR images; those having higher coherence (>0.92) yielded accurate results. As the coherence decreased, it was not feasible to proceed with the SAR images. Every image is used as a master image once, with respect to rest of the images as slave mentioned in Table 3. The estimated velocity with different images is graphically represented in Figure 4.

Table 3. Velocity output estimated using different images.

Date of Image	Average Coherence (0 to 1)	Estimated Average Velocity (ma^{-1})
07-08-2016	0.76	432
19-08-2016	0.78	441
31-08-2016	0.81	442
12-09-2016	0.65	465
30-09-2016	0.82	476
18-10-2016	0.92	513
24-10-2016	0.90	528
05-11-2016	0.92	576
11-11-2016	0.94	580
17-11-2016	0.93	586
05-12-2016	0.88	580
11-12-2016	0.68	580
29-12-2016	0.79	582
04-01-2017	0.79	583
22-01-2017	0.78	524
21-02-2017	0.68	520

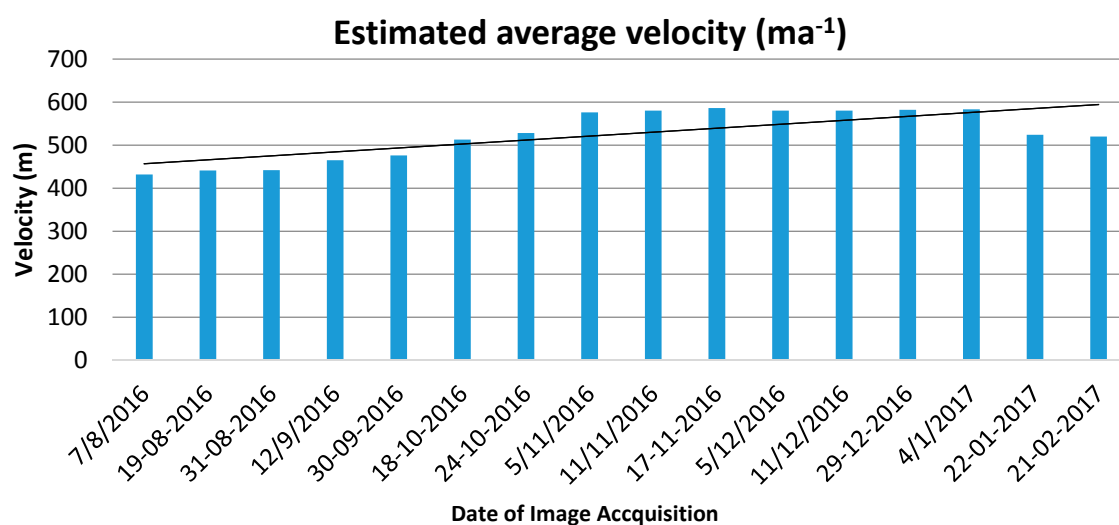


Figure 4. Estimated average velocity (ma⁻¹).

Acknowledgments: The authors would like to thank Daniele Perissin, Assistant Professor at Purdue University for providing the software assistance. We are very thankful to the European Space Agency for making availability Sentinel-1 data for free. We also acknowledge M. Ravichandran, Director, ESSO-NCAOR, for his encouragement and motivation for this research.

Conflicts of Interest: The authors declare no conflicts of interest.

Abbreviations

The following abbreviations are used in this manuscript:

PRG	Polar Record Glacier
SAR	Synthetic Aperture Radar
DEM	Digital Elevation Model
SLC	Single Look Complex
DInSAR or DiffSAR	Differential SAR interferometry
PSI or PSInSAR	Persistent scatterer interferometry

References

1. Goldstein, R.M.; Werner, C. Radar interferogram filtering for geophysical applications. *Geophys. Res. Lett.* **1998**, *25*, 4035–4038.
2. Massonnet, D.; Feigl, K. Radar interferometry and its application to changes in the Earth's surface. *Rev. Geophys.* **1998**, *36*, 441–500.
3. Berardino, P.; Fornaro, G.; Lanari, R.; Sansosti, E. A new algorithm for surface deformation monitoring based on small baseline differential SAR interferograms. *IEEE Trans. Geosci. Remote Sens.* **2002**, *40*, 2375–2383.
4. Kenyi, L.; Kaufmann, V. Estimation of rock glacier surface deformation using SAR interferometry Data. *IEEE Trans. Geosci. Remote Sens.* **2003**, *41*, 1512–1515.
5. Berthier, E.; Vadon, H.; Baratoux, D.; Arnaud, Y.; Vincent, C.; Feigl, K.; Rémy, F.; Legrésy, B. Surface motion of mountain glaciers derived from satellite optical imagery. *Remote Sens. Environ.* **2005**, *95*, 14–28.
6. Strozzi, T.; Luckman, A.; Murray, T.; Wegmuller, U.; Werner, C. Glacier motion estimation using SAR offset-tracking procedures. *IEEE Trans. Geosci. Remote Sens.* **2002**, *40*, 2384–2391.
7. Dietrich, R.; Metzger, R.; Korth, W.; Perlt, J. Combined use of field observations and SAR interferometry to study ice dynamics and mass balance in Dronning Maud Land, Antarctica. *Polar Res.* **1999**, *18*, 291–298.

8. Zhou, C.; Zhou, Y.; Deng, F.; Ai, S.; Wang, Z.; Dongchen, E. Seasonal and interannual ice velocity changes of Polar Record Glacier, East Antarctica. *Ann. Glaciol.* **2014**, *55*, 45–51.
9. Anschütz, H.; Eisen, O.; Oerter, H.; Steinhage, D.; Scheinert, M. Investigating small-scale variations of the recent accumulation rate in coastal Dronning Maud Land, East Antarctica. *Ann. Glaciol.* **2007**, *46*, 14–21.
10. Bürgmann, R.; Rosen, P.; Fielding, E. Synthetic Aperture Radar Interferometry to Measure Earth's Surface Topography and Its Deformation. *Annu. Rev. Earth Planet. Sci.* **2000**, *28*, 169–209.
11. Ferretti, A.; Prati, C.; Rocca, F. Nonlinear subsidence rate estimation using permanent scatterers in differential SAR interferometry. *IEEE Trans. Geosci. Remote Sens.* **2000**, *38*, 2202–2212.
12. Hellwich, O.; Ebner, H. Geocoding SAR interferograms by least squares adjustment. *ISPRS J. Photogramm. Remote Sens.* **2000**, *55*, 277–288.
13. Jawak, S.D.; Bidawe, T.; Luis, A. A Review on Applications of Imaging Synthetic Aperture Radar with a Special Focus on Cryospheric Studies. *Adv. Remote Sens.* **2015**, *4*, 163–175.
14. Jawak, S.D.; Luis, A.J. Prospective application of NASA-ISRO SAR (NISAR) in cryospheric studies: A practical approach. In Proceedings of the NISAR Science Workshop, Space Applications Centre (SAC), Ahmedabad, Gujarat, India, 17–18 November 2014.



© 2018 by the authors. Licensee MDPI, Basel, Switzerland. This article is an open access article distributed under the terms and conditions of the Creative Commons Attribution (CC BY) license (<http://creativecommons.org/licenses/by/4.0/>).